Korean J. Chem. Eng., **31**(2), 194-200 (2014)
DOI: 10.1007/s11814-013-0212-7

pISSN: 0256-1115
eISSN: 1975-7220

Simulation of a bubbling fluidized bed process for capturing CO_2 from flue gas

Jeong-Hoo Choi*,†, Chang-Keun Yi, Sung-Ho Jo**, Ho-Jung Ryu**, and Young-Cheol Park****

*Department of Chemical Engineering, Konkuk University, 1 Hwayang-dong, Gwangjin-gu, Seoul 143-701, Korea
**Korea Institute of Energy Research, 71-2, Jang-dong, Yuseong-gu, Daejeon 305-343, Korea
(*Received 21 June 2013 • accepted 14 October 2013*)

Abstract−We simulated a bubbling bed process capturing CO_2 from flue gas. It applied for a laboratory scale process to investigate effects of operating parameters on capture efficiency. The adsorber temperature had a stronger effect than the regenerator temperature. The effect of regenerator temperature was minor for high adsorber temperature. The effect of regenerator temperature decreased to level off for the temperature >250 °C. The capture efficiency was rather dominated by the adsorption reaction than the regeneration reaction. The effect of gas velocity was as appreciable as that of adsorber temperature. The capture efficiency increased with the solids circulation rate since it was ruled by the molar ratio of K to CO_2 for solids circulation smaller than the minimum required one ($G_{s,min}$). However, it leveled off for solids circulation rate >$G_{s,min}$. As the ratio of adsorber solids inventory to the total solids inventory (x_{w1}) increased, the capture efficiency increased until x_{w1}=0.705, but decreased for x_{w1}>0.705 because the regeneration time decreased too small. It revealed that the regeneration reaction was faster than the adsorption reaction. Increase of total solids inventory is a good way to get further increase in capture efficiency.

Keywords: CO_2 Capture, Flue Gas, Simulation, Fluidized Bed, Dual Bed

INTRODUCTION

Accumulation of CO_2 in the atmosphere is recognized as one of important causes accelerating global warming. Many studies have accordingly been carried out for processes to capture CO_2 from flue gas massively by using solid sorbents based on Na, K, and Ca [1-16].

The fluidized-bed CO_2 capture system has several potential advantages. The fluidized bed provides good solids mixing for gas-solids contact and heat transfer between bed and immersed heat exchanger tubes. Adsorption for CO_2 capture is exothermic, while desorption for regeneration of sorbent is endothermic. It is good to maintain uniform temperature distribution with heat transfer, and therefore is easier to operate than the fixed bed reactor. A mathematical simulation can provide a tool for investigating effects of various operating parameters on the reactor performance in advance. It serves as a cost, time, and efforts saver in systematic understanding of experimental results, process design, and process operation. There have only been a few available reports on steady state analysis of the present process [14,16]. Choi et al. [14] developed a model for an entrained-bed adsorber and bubbling-bed regenerator system that used Na-based regenerable sorbent. They developed a particle population balance for both reactors and combined it with reaction rates on adsorption and regeneration for predicting the CO_2 capture efficiency. Choi et al. [16] also carried out the same kind of work on a bubbling-bed adsorber and regenerator system based on the study of Kim et al. [13]. The model fitted the experimental data [13] well on effects of gas velocity, temperature, and H_2O content of the adsorber, and temperature of the regenerator. However, it mainly focused on testing the model's suitability on parametric effects. In addition, effects of solids circulation rate [13] and concentration of both CO_2 and H_2O in the regenerator [15] were not understood well.

The purpose of this study was to improve the model of Choi et al. [16] for fitting the effect of CO_2 concentration in the regenerator [15] and to carry out detail simulation on effects of operating parameters on the CO_2 capture efficiency. The simulation was carried out for the laboratory scale bubbling bed process of Korea Institute of Energy Research (KIER) [13,15] that used a K-based regenerable sorbent.

MODEL

Fig. 1 shows the schematic diagram of the process considered in this study, which uses a bubbling-bed adsorber and a bubbling-bed

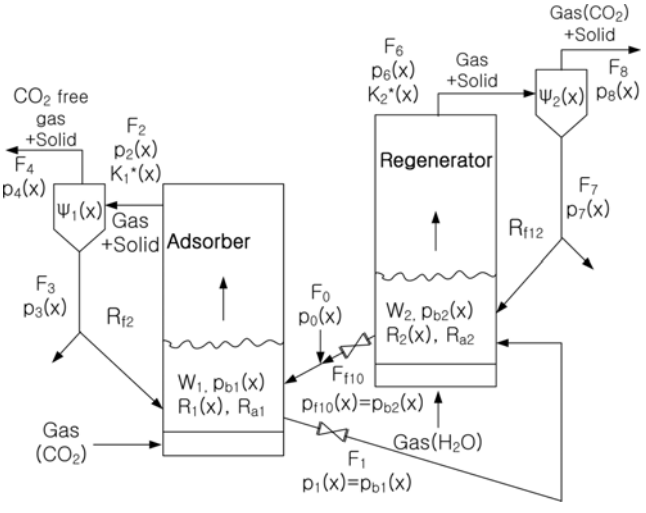

Fig. 1. Flow diagram of a bubbling bed CO_2 capture process.

†To whom correspondence should be addressed.
E-mail: choijhoo@konkuk.ac.kr

regenerator. Flue gas containing CO_2 is introduced to the adsorber and fluidizes the bed of sorbent particles. Potassium-based sorbent particles were used to adsorb CO_2 according to the following reaction

$$K_2CO_3(s)+CO_2(g)+H_2O(g)=2KHCO_3(s) \quad (1)$$

Reacted sorbent particles are withdrawn from the adsorber and sent to the regenerator. Entrained particles are collected by a cyclone, and returned to the reactor ($R_{f12}=R_{f2}=1$). Steam or other gas is introduced to the regenerator and fluidizes the bed of sorbent particles. Sorbent particles containing CO_2 are regenerated according to the reverse reaction. Regenerated sorbent particles are returned to the adsorber. The fractional collection efficiency of the cyclone ($\psi_i(x)$) is assumed as that of Lapple [17]. We assumed a well-mixed state of bed particles in both reactors ($p_1(x)=p_{b1}(x)$, $p_{f10}(x)=p_{b2}(x)$). The steady state particle population balance in the adsorber (i=1) and regenerator (i=2) gives [14,16]

$$\frac{dp_{bi}(x)}{dx}+\sum_{k=1}^{2}\alpha_{ik}(x)p_{bk}(x)-\alpha_{i3}(x)=0 \quad (i=1, 2) \quad (2)$$

$$\alpha_{i1}(x)=\delta_{1i}\left[\frac{F_1+K_1^*(x)(1-\psi_1(x)R_{f12})}{W_1R_1(x)}+\frac{1}{R_1(x)}\frac{dR_1(x)}{dx}-\frac{3}{x}\right]-\delta_{2i}\frac{F_1}{W_2R_2(x)} \quad (3)$$

$$\alpha_{i2}(x)=-\delta_{1i}\frac{F_{f10}}{W_1R_1(x)}+\delta_{2i}\left[\frac{F_{f10}+K_2^*(x)(1-R_{f2}\psi_2(x))}{W_2R_2(x)}+\frac{1}{R_2(x)}\frac{dR_2(x)}{dx}-\frac{3}{x}\right] \quad (4)$$

$$\alpha_{i3}(x)=-\frac{\delta_{1i}F_0p_0(x)+R_{ai}p_{ai}(x)}{W_iR_i(x)} \quad (5)$$

$$\text{B. C.: } p_{bi}(x)=0 \text{ for } x=x_{max} \quad (6)$$

$$\text{Constraint: } \int_0^{x_{max}}p_{bi}(x)dx=1 \quad (7)$$

The δ_{ij} is the Kronecker delta. We used correlations of Choi et al. [18] for the particle entrainment rate $K_i^*(x)$ and the model of Merrick and Highley [19] for attrition rates R_{ai} and $R_i(x)$:

$$R_{ai}=K_a(u_i-u_{mfi})W_i \quad (8)$$

$$R_i(x)=dx/dt=-K_a(u_i-u_{mfi})x/3 \quad (9)$$

We assumed that fine particles formed by abrasion had diameter <5 mm, a uniform size distribution, and negligible attrition.

The population balance in each reactor from Eqs. (2) to (9) was solved by the finite difference method and it determined the particle size distribution of bed i, $\omega_{bi}(d_p)$. Reaction time of particles of a size was considered as their mean residence time in each reactor [20] by

$$\tau_i(d_p)=\frac{W_{bi}\omega_{bi}(d_p)}{\sum_{j(out\text{-}flows)}S_{ij}\omega_{ij}(d_p)} \quad (10)$$

Retention times in both reactors were used in Eqs. (14) and (17) to determine conversions of adsorption and desorption. It is impossible to represent mathematically the exact gas flow pattern in the fluidized bed and the contacting pattern between gas and solid particles. Both adsorption and regeneration reactions participating CO_2 and H_2O may mainly take place in particles close to the particle surface. The exact reaction mechanism is also very difficult to express mathematically. As a result, the final tune-up employing correction for any choice of reaction mechanism should be done with some sets of experimental data. Therefore, the present model [16] took as simple choices as possible only for the bubbling fluidization regime on average concentration of gas reactant, reaction mechanism, and reaction time.

Table 1. Size distribution of fresh sorbent particles

Sieve size [μm]	0-63	63-75	75-106	106-150	150-212	212-350
Mass fraction	0.074	0.069	0.301	0.407	0.143	0.0006

The average concentration of gas in each reactor was simply considered as an arithmetic mean value between inlet and outlet concentration.

$$\overline{C_{ij}}=\frac{C_{ij,0}+C_{ij,f}}{2} \quad (11)$$

We modified the order of reaction on CO_2 in regeneration [16] by trial-and-error with four sets of experimental data (Table 1 and Fig. 3 in the study of Kim et al. [15]) on the effect of CO_2 concentration of regenerator on CO_2 capture efficiency. During this process, the activation energy of regeneration and other two proportional constants also changed a little by the same way, reconsidering experimental data (Table 3 and Figs. 5 to 9 in the study of Kim et al. [13]) that were used for the previous model [16]. The average relative error was 9.37% and 8.23% for previous and present models, respectively.

$$\frac{dX}{dt}=\frac{1.690\times10^{-7}(1-X)^{2/3}}{d_p}e^{-E_1/RT_1}\overline{C_{CO_2}}\overline{C_{H_2O}},$$

$$E_1=-22.49 \text{ kJ/g mol} \quad (12)$$

$$\text{B. C.: } X=X_{1i}(d_p) \text{ at } t=0 \quad (13)$$

$$X=X_{1f}(d_p) \text{ at } t=\tau_1(d_p) \quad (14)$$

$$\frac{d\lambda}{dt}=\frac{2.433\times10^{-9}(1-\lambda)^{2/3}}{d_p}e^{-E_2/RT_2}\frac{1}{\overline{C_{CO_2}}(\overline{C_{H_2O}})^{1.06}},$$

$$E_2=46.03 \text{ kJ/g mol} \quad (15)$$

$$\text{B. C.: } \lambda=0,\ X=X_{2i}(d_p) \text{ at } t=0 \quad (16)$$

$$\lambda=\lambda_f(d_p),\ X=X_{2f}(d_p)=X_{1f}(d_p)(1-\lambda_f(d_p)) \text{ at } t=\tau_2(d_p) \quad (17)$$

Reaction rates considered for average particle size and average particle retention time.

The following relations between moles of CO_2 and moles of $KHCO_3$ (formed and disappeared) must be satisfied in each reactor:

$$\Delta N_{1,KHCO_3}=-2\Delta n_{1,CO_2} \quad (18)$$

$$\Delta N_{2,KHCO_3}=-2\Delta n_{2,CO_2} \quad (19)$$

By combining Eqs. (2) to (19), the present model can calculate the particle flow rate, particle size distribution, concentration of CO_2 in gas phase and $KHCO_3$ in particles. The overall capture efficiency of CO_2 can be determined from the mole balance on CO_2.

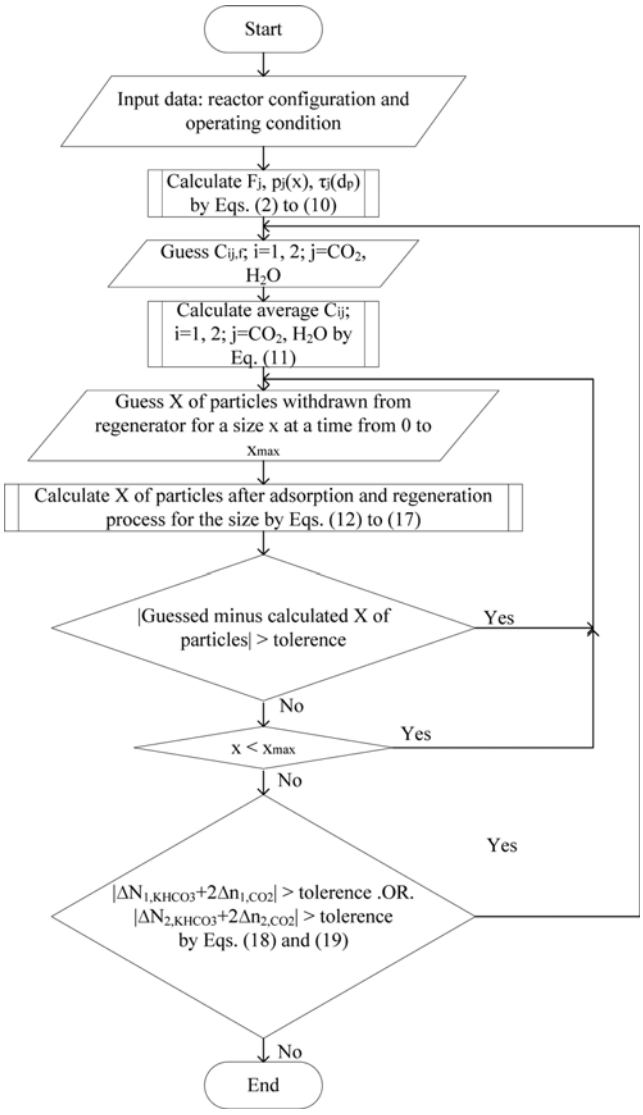

Fig. 2. Flow chart on model calculation procedure.

CALCULATION PROCEDURE

Fig. 2 depicts the flow chart on model calculation procedure. Mass flow rates and size distributions of all particle streams are calculated by combining Eqs. (2) to (9) with the finite difference method. The average residence time for a particle size in each reactor ($\tau_1(d_p)$, $\tau_2(d_p)$ for Eqs. (14) and (17)) is calculated by Eq. (10). An initial educated guess for outlet concentrations of CO_2 and H_2O in adsorber and regenerator ($C_{ij,f}$, i=1, 2; j=CO_2, H_2O) determines adsorbing and desorbing rate of CO_2 ($\Delta n_{1,CO_2}$, $\Delta n_{2,CO_2}$) for Eqs. (18) and (19), and average concentration of each gas (C_{ij}, i=1, 2; j=CO_2, H_2O) in each reactor by Eq. (11). The adsorption conversion X for a particle size in each reactor is calculated as follows: 1) Make a best guess for adsorption conversion $X_{2f}(d_p)$ of particle withdrawn from the regenerator in Eq. (17). The particle is sent to the adsorber, then $X_{1i}(d_p)=X_{2f}(d_p)$ in Eq. (13). 2) Evaluate $X_{1f}(d_p)$ of the particle in Eq. (14) by Eqs. (12) to (14) when it is withdrawn from the adsorber after reaction time of mean residence time $\tau_1(d_p)$ from Eq. (10). The particle is returned to the regenerator, then $X_{2i}(d_p)=X_{1f}(d_p)$ in Eq. (16). 3) Evaluate new $X_{2f}(d_p)$ of the particle withdrawn from the regenerator in Eq. (17) by Eqs. (15) to (17) after reaction time of mean residence time $\tau_2(d_p)$ from Eq. (10). 4) See if the difference between the new adsorption conversion $X_{2f}(d_p)$ of the particle from the regenerator and the one initially guessed in step 1 is within tolerance. If not, go back to step 1 and make another educated guess from the results. Use the same calculation for all particle sizes. As a result, we can obtain the total mole flow rate of CO_2 adsorbed by particles from the gas phase in the adsorber ($\Delta N_{1,KHCO_3}/2$) and the total mole flow rate of CO_2 released from particles to the gas phase in the regenerator ($\Delta N_{2,KHCO_3}/2$) for Eqs. (18) and (19). Eqs. (18) and (19) between moles of CO_2 (adsorbed or desorbed) and moles of $KHCO_3$ (formed or disappeared) in each reactor must be satisfied. Continue with best guesses for outlet concentration of CO_2 in the adsorber and the regenerator to narrow the differences until Eqs. (18) and (19) are satisfied within tolerance.

SIMULATION CONDITIONS

The present model was applied to the KIER process (adsorber: 0.11 m i.d., 1.2 m height; regenerator: 0.11 m i.d., 1.2 m height) [13, 15]. Table 1 summarizes the size distribution of fresh sorbent. The specific surface mean diameter was 99.5 μm. The apparent particle density was 1640 kg/m^3. It had 5.07×10^{-3} kg mol potassium/kg solid. The minimum fluidizing velocity was 8.8 mm/s at ambient temperature and pressure. Gas mixture of N_2, H_2O and CO_2 was used as fluidizing gas for the adsorber and the regenerator. The fluidizing gas for the adsorber maintained the mole ratio of N_2 to CO_2 as 9/1. The following settings were held constant: pressure, 101.3 kPa; attrition coefficient of particle=3×10^{-9}/mm.

RESULTS AND DISCUSSION

The CO_2 capture efficiency was estimated by a mole balance on CO_2 in the adsorber. Captured moles of CO_2 were determined as difference in mole flow rate of CO_2 between gas inlet and outlet of the adsorber. It was checked well by the mole flow rate of CO_2 at

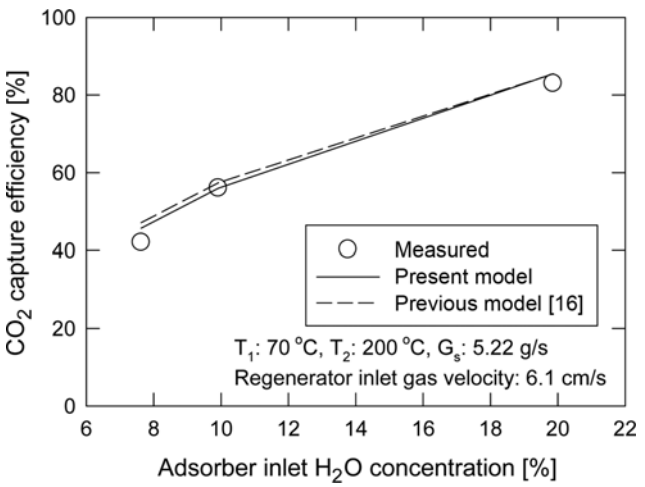

Fig. 3. Effect of moisture concentration of adsorber gas on CO_2 capture efficiency (symbol: measured by Kim et al. [13], lines: simulations).

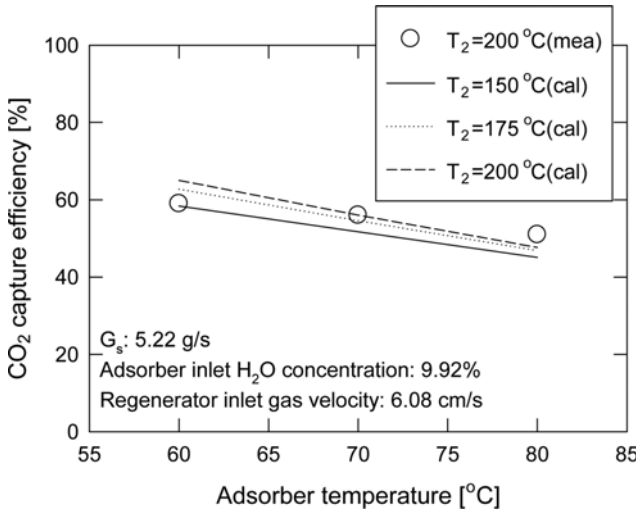

Fig. 4. Effect of adsorber temperature on CO_2 capture efficiency (symbol: measured by Kim et al. [13], lines: simulation).

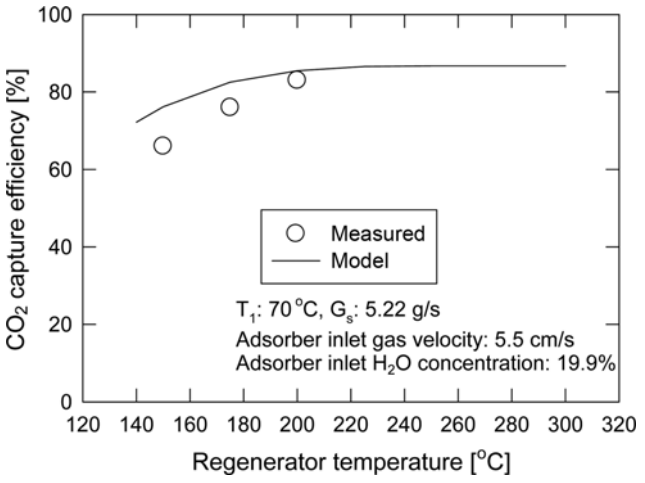

Fig. 5. Effect of regenerator temperature on CO_2 capture efficiency (symbol: measured by Kim et al. [13], lines: simulation).

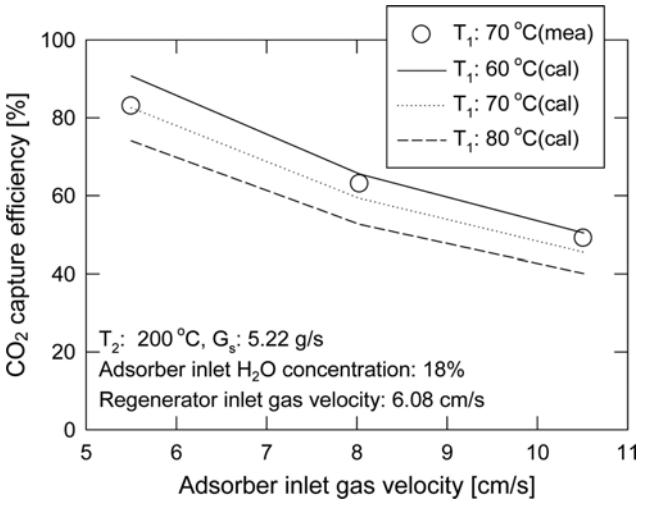

Fig. 6. Effect of adsorber inlet gas velocity on CO_2 capture efficiency (symbol: measured by Kim et al. [13], lines: simulation).

the gas outlet of the regenerator. The CO_2 capture efficiency was a ratio of captured moles of CO_2 to feed moles of CO_2 for the adsorber.

Fig. 3 shows the effect of moisture content of the feed gas to the adsorber on CO_2 capture efficiency and compares the measured value [13] with the one calculated by previous [16] and present models. Temperature was 70 °C for the adsorber and 200 °C for the regenerator. The solids circulation rate was 5.2 g/s. The inlet fluidizing velocity was 0.0608 m/s for the regenerator. But the inlet fluidizing gas velocity for the adsorber increased from 0.0477 to 0.0550 m/s as the moisture content increased. The CO_2 capture efficiency increased as the moisture content increased, because the adsorption reaction rate increased as the reactant moisture concentration increased [1,14]. We confirmed that this model fairly agreed with the previous one [16].

Fig. 4 depicts the effect of adsorber temperature on CO_2 capture efficiency and compares the measured value [13] with the one calculated by the present model for 200 °C regenerator temperature. The moisture content of the feed gas to the adsorber was 9.92%. The solids circulation rate was 5.2 g/s. The inlet fluidizing velocity was 0.0489 m/s for the adsorber and 0.0608 m/s for the regenerator. The CO_2 capture efficiency decreased as the temperature increased. The equilibrium of adsorption reaction moves to the reverse direction as the adsorber temperature increases because of the exothermic nature of adsorption reaction [1,14]. Therefore, the capture efficiency decreased. On the other hand, the capture efficiency increased as the regenerator temperature increased, due to the endothermic nature of the desorption reaction. However, the effect of regenerator temperature decreased as the adsorber temperature increased. Adsorber temperature had a stronger effect than regenerator temperature.

Fig. 5 indicates the effect of regenerator temperature on CO_2 capture efficiency with comparison between the measured value [13] and the one calculated by the present model. Temperature was 70 °C for the adsorber. The moisture content of the feed gas to the adsorber was 19.9%. The solids circulation rate was 0.0052 kg/s. The inlet fluidizing gas velocity was 0.055 m/s for the adsorber and 0.0576 m/s for the regenerator. The CO_2 capture efficiency increased as the temperature increased. The equilibrium of regeneration reaction moved to the forward direction as the regenerator temperature increased because the regeneration reaction was endothermic. Then K_2CO_3 concentration in solids returned to the adsorber increased, the adsorption reaction rate was promoted, and therefore the capture efficiency increased [1,14]. However, the slope of increase was predicted to decrease and level off for a temperature >250 °C. The capture efficiency seemed to be dominated by the adsorption reaction.

Fig. 6 shows the effect of the inlet fluidizing velocity of the adsorber on CO_2 capture efficiency and compares the measured value [13] with the one calculated by the present model. Temperature was 70 °C for the adsorber and 200 °C for the regenerator. The solids circulation rate was 0.0052 kg/s. The fluidizing gas velocity was 0.0608 m/s for the regenerator. The CO_2 capture efficiency decreased as the fluidizing gas velocity increased, because the retention time of the gas phase decreased as the gas velocity increased [14]. The effect of gas velocity seemed to be as appreciable as that of temperature, as can be seen in Fig. 6.

Fig. 7 shows the effect of the solids circulation rate on CO_2 capture

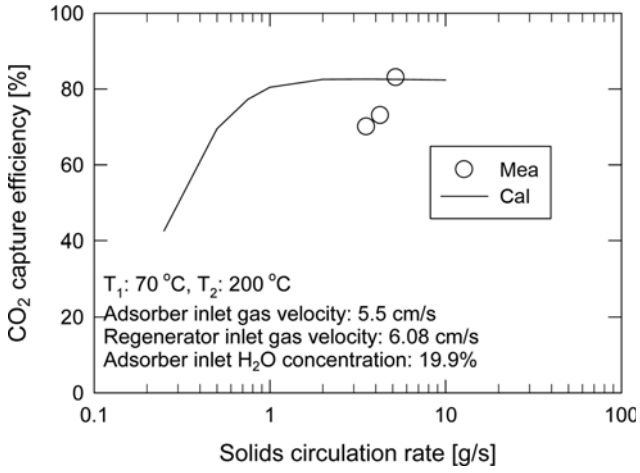

Fig. 7. Effect of solids circulation rate on CO_2 capture efficiency (symbol: measured by Kim et al. [13], line: simulation).

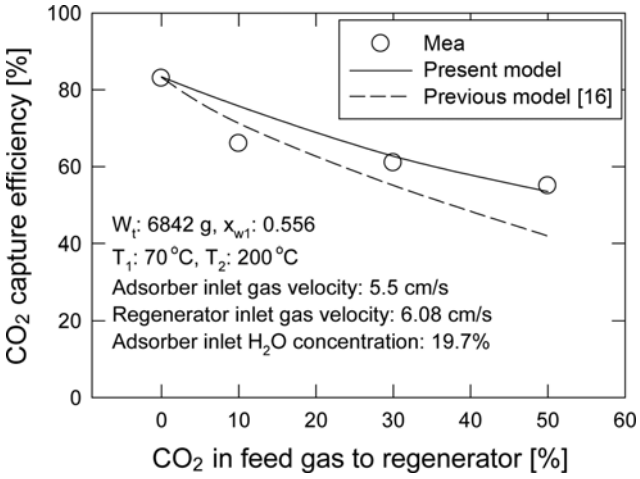

Fig. 9. Effect of CO_2 concentration in regenerator on CO_2 capture efficiency (symbol: measured by Kim et al. [15], lines: simulations).

efficiency with comparison between the measured value [13] and the one calculated by the present model. Temperature was 70 °C for the adsorber and 200 °C for the regenerator. The moisture content of the feed gas to the adsorber was 19.9%. The inlet fluidizing gas velocity was 0.0550 m/s for the adsorber and 0.0608 m/s for the regenerator. The CO_2 capture efficiency measured in experiment increased as the solids circulation rate increased. The efficiency predicted by the model increased but the slope decreased and leveled off for solids circulation rate >0.002 kg/s (molar ratio of K to CO_2= 6.81) that we called minimum required solids circulation ($G_{s,min}$). The capture efficiency was dominated by the molar ratio of K to CO_2 at solids circulation <$G_{s,min}$. The capture efficiency increased with the solids circulation rate. However, the capture efficiency became nearly constant for solids circulation rate >$G_{s,min}$. Thus, the model seemed to predict the $G_{s,min}$ smaller than the measured value 0.0052 kg/s [13] since the model assumed a well mixed bed. The solids flow pattern in the bed can be affected by fluidizing conditions, geometry and configuration of solids inlet and outlet. Further improvement is needed for this model to reflect this effect correctly.

Fig. 8(a) indicates the effect of solids inventory ratio of adsorber to total solids inventory (x_{w1}) on the CO_2 capture efficiency. The total solids inventory of the process was 7.27 kg. The increase of adsorber solids inventory meant a decrease of the regenerator solids inventory. As the x_{w1} increased, the effect was marginal on capture efficiency increasing until x_{w1}=0.705 but decreasing for x_{w1}>0.705 in the present condition because the regeneration time decreased too small. It also meant the regeneration reaction was faster than the adsorption reaction. Fig. 8(b) indicates the effect of total solids inventory on the CO_2 capture efficiency. Both reaction times of adsorption and desorption increased and resulted in an increase of capture efficiency as the total solids inventory increased. The capture efficiency was predicted 100% for the total solids inventory 10.8 kg. Therefore, increase of total solids inventory could be a good choice in order to get further increase in capture efficiency.

Fig. 9 shows the effect of CO_2 concentration in the regenerator on the CO_2 capture efficiency. The regeneration was interrupted by the reverse reaction, adsorption of CO_2, increasing with an increase of CO_2 concentration, and therefore the CO_2 capture efficiency decreased [15]. The effect of H_2O concentration on CO_2 capture was

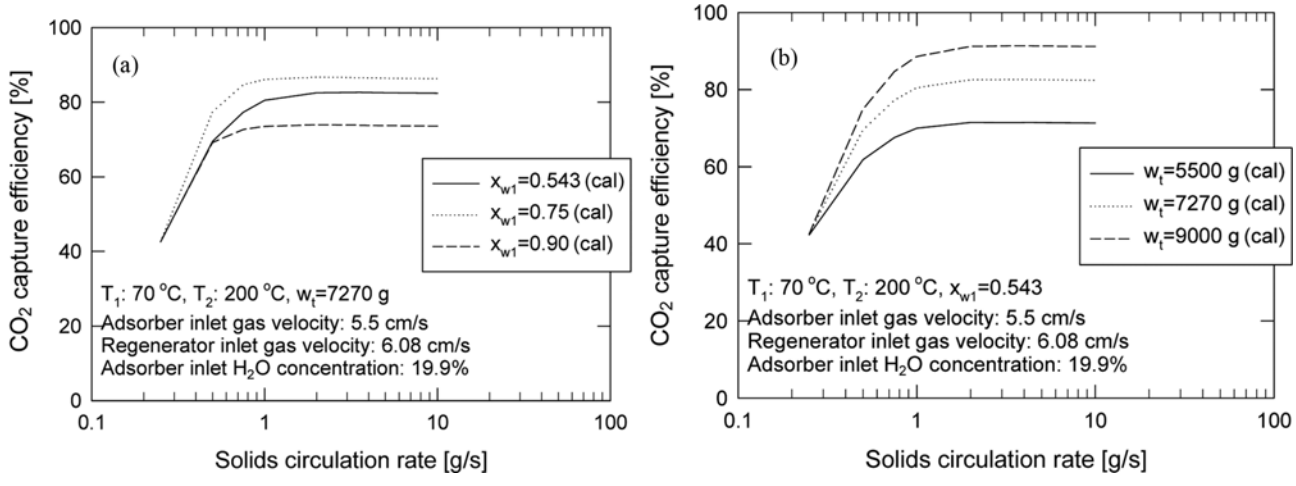

Fig. 8. Effects of solids inventory and its distribution on CO_2 capture efficiency (lines: simulation).

not predicted properly. The CO_2 capture efficiency increased [15]; however, the present model predicted it to decrease because the reverse reaction, adsorption of CO_2, increased as the H_2O concentration increased. Further study on desorption mechanism in the regenerator is needed to explain this effect properly.

CONCLUSIONS

We simulated effects of some operating parameters on capture efficiency of a bubbling bed process capturing CO_2 from flue gas and reached the following conclusions.

The effect of regenerator temperature decreased as the adsorber temperature increased. The effect of adsorber temperature was stronger than that of regenerator temperature. The effect of regenerator temperature was predicted to decrease and level off for the temperature >250 °C. The capture efficiency was rather dominated by the adsorption reaction than the regeneration reaction. The effect of gas velocity was as appreciable as that of adsorber temperature. The capture efficiency was predicted to increase with the solids circulation rate since it was dominated by the molar ratio of K to CO_2 for solids circulation smaller than the minimum required one ($G_{s,min}$). However, it leveled off for solids circulation rate >$G_{s,min}$. As the ratio of adsorber solids inventory to the total solids inventory (x_{w1}) increased, the capture efficiency increased until x_{w1}=0.705, but decreased for x_{w1}>0.705 in the present condition because the regeneration time decreased too little. It revealed that the regeneration reaction was faster than the adsorption reaction. Increase of total solids inventory is a good way in order to get complete capture efficiency. The predicted effect of CO_2 concentration in the regenerator on capture efficiency agreed with the measured value reasonably well. However, further study on the regeneration mechanism is needed to explain the measured capture efficiency [15] that increased with the moisture concentration in the regenerator.

ACKNOWLEDGEMENTS

This work was supported by the Energy Efficiency & Resources of the Korea Institute of Energy Technology Evaluation and Planning (KETEP) grant funded by the Korea government Ministry of Knowledge Economy (2010T100200344).

NOMENCLATURE

$\overline{C_{CO_2}}$, $\overline{C_{H_2O}}$: average concentration of gaseous reactants CO_2 and H_2O in reactor, respectively [kg mol/m^3]
$C_{ij,o}$, $C_{ij,f}$, $\overline{C_{ij}}$: inlet, outlet, and average concentration of gaseous reactant j (CO_2, H_2O) in reactor i [kg mol/m^3]
d_p : particle diameter [m]
E_i : activation energy of reaction i [kJ/g mol]
F_j : solid flow rate of stream j [kg/s]
G_s : solids circulation rate [kg/s]
$G_{s,min}$: minimum required solids circulation rate for its effect leveling off [kg/s]
K_a : particle attrition rate constant [1/m]
$K_i^*(x)$: particle elutriation rate from bed i [kg/s]
$\Delta N_{i,KHCO_3}$: total moles of $KHCO_3$ in inflow of solids minus outflow of solids [kg mol/s]
$\Delta n_{i,CO_2}$: total moles of CO_2 in inflow of gas minus outflow of gas [kg mol/s]
$p_{ai}(x)$: probability density function of particles formed by attrition in bed i [1/m]
$p_{bi}(x)$: probability density function of particles in bed i [1/m]
$p_j(x)$: probability density function of particles in stream j [1/m]
$p_0(x)$: probability density function of fresh feed particles [1/m]
R : gas constant, 8.314 [kPa m^3/kg mol K]
R_{ai} : overall formation rate of fine particles by attrition in bed i [kg/s]
R_{fi} : recycle fraction of solid collected by cyclone [-]
$R_i(x)$: particle attrition rate in bed i [m/s]
S_{ij} : mass flow rate of total particle in outflow stream j from bed i [kg/s]
t : time [s]
T : temperature [K]
u_i : arithmetic average fluidizing gas velocity in reactor i [m/s]
u_{mfi} : minimum fluidizing gas velocity in reactor i [m/s]
W_i : weight of bed i [kg]
W_t : total solids inventory in both adsorber and regenerator [kg]
x, x_{max} : spherical particle diameter and maximum x [m]
X : conversion of K_2CO_3 to $KHCO_3$ in solids [-]
X_{ii}, X_{if} : conversion of K_2CO_3 to $KHCO_3$ for in- and out-flow of reactor i [-]
x_{w1} : ratio of adsorber solids inventory to total solids inventory [-]

Greeks

α_{ik}, α_{i3} : functions defined as Eqs. (3) to (5) [1/m, 1/m^2]
δ_{ij} : Kronecker delta [-]
λ : conversion of regeneration reaction [-]
λ_f : conversion of regeneration reaction of solids discharged from regenerator [-]
τ_i : mean particle residence time in reactor [s]
$\psi_i(x)$: cyclone collection efficiency [-]
$\varpi_{bi}(d_p)$: mass fraction of particle in bed i [-]
$\varpi_{ij}(d_p)$: mass fraction of particle in outflow stream j from bed i [-]

Subscripts

b : bed
i : free index, 1 for adsorber and 2 for regenerator
j, k : indices

REFERENCES

1. C. K. Yi, S. W. Hong, S. H. Jo, J. E. Son and J.-H. Choi, *Korean Chem. Eng. Res.*, **43**, 294 (2005).
2. C.-K. Yi, S.-H. Jo, Y. Seo, J.-B. Lee and C.-K. Ryu, *Int. J. Greenhouse Gas Control*, **1**, 31 (2007).
3. J. B. Lee, C. K. Ryu, J.-I. Baek, J. H. Lee, T. H. Eom and S. H. Kim, *Ind. Eng. Chem. Res.*, **47**, 4465 (2008).
4. C.-K. Yi, S.-H. Jo and Y. Seo, *J. Chem. Eng. Jpn.*, **41**, 691 (2008).
5. J. C. Abanades, M. Alonso, N. Rodriguez, B. Gonzalez, G. Grasa and R. Murillo, *Energy Procedia*, **1**, 1147 (2009).
6. M. Alonso, N. Rodriguez, G. Grasa and J. C. Abanades, *Chem. Eng. Sci.*, **64**, 883 (2009).

7. F. Fang, Z. Li and N. Cai, *Ind. Eng. Chem. Res.*, **48**, 11140 (2009).
8. K.-W. Park, Y. S. Park, Y. C. Park, S.-H. Jo and C.-K. Yi, *Korean Chem. Eng. Res.*, **47**, 349 (2009).
9. Y. C. Park, S.-H. Jo, K.-W. Park, Y. S. Park and C.-K. Yi, *Korean J. Chem. Eng.*, **26**, 874 (2009).
10. Y. Seo, S.-H. Jo, C. K. Ryu and C.-K. Yi, *J. Environ. Eng.*, **135**, 473 (2009).
11. J. Stroehle, A. Lasheras, A. Galloy and B. Epple, *Chem. Eng. Technol.*, **32**, 435 (2009).
12. C.-K. Yi, *Korean Chem. Eng. Res.*, **48**, 140 (2010).
13. K.-C. Kim, K.-Y. Kim, Y. C. Park, S.-H. Jo, H.-J. Ryu and C.-K. Yi, *Korean Chem. Eng. Res.*, **48**, 499 (2010).
14. J.-H. Choi, C.-K. Yi and S.-H. Jo, *Korean J. Chem. Eng.*, **28**, 1144 (2011).
15. K.-C. Kim, Y. C. Park, S.-H. Jo and C.-K. Yi, *Korean J. Chem. Eng.*, **28**, 1986 (2011).
16. J.-H. Choi, P. S. Youn, K.-C. Kim, C.-K. Yi, S.-H. Jo, H.-J. Ryu and Y.-C. Park, *Korean Chem. Eng. Res.*, **50**, 516 (2012).
17. C. E. Lapple, *Chem. Eng.*, **58**, 144 (1951).
18. J. H. Choi, I. Y. Chang, D. W. Shun, C. K. Yi, J. E. Son and S. D. Kim, *Ind. Eng. Chem. Res.*, **38**, 2491 (1999).
19. D. Merrick and J. Highley, *AIChE Symp. Ser.*, **70**, 366 (1974).
20. D. Kunii and O. Levenspiel, *Fluidization engineering*, 2nd Ed., Butterworth-Heinemann, Boston (1991).